In the jaws of a titan: 3D comparative anatomy of the mandibles of the Canary giant lizards (Gallotiinae: *Gallotia*)

Pérez-Martín, S.[1], Fortuny, J.[2], Cruzado-Caballero, P.[*,1,3,4,5], Bernardini, F.[6,7], and Castillo Ruiz, C.[1]

[1]Área de Paleontología, Departamento de Biología Animal, Edafología y Geología, Universidad de La Laguna, Av. astrofísico Francisco Sánchez, 2, 38206, San Cristóbal de La Laguna, Santa Cruz de Tenerife, Spain; sprezmart@gmail.com; ccruiz@ull.edu.es, pcruzado@ull.edu.es

[2]Institut Català de Paleontologia Miquel Crusafont, Universitat Autònoma de Barcelona, Edifici ICTA-ICP, C/ Columnes s/n, Campus de la UAB, 08193 Cerdanyola del Vallès, Barcelona, Spain. josep.fortuny@icp.cat

[3]Universidad Nacional de Río Negro. Instituto de Investigación en Paleobiología y Geología, Río Negro, Argentina.

[4]IIPG. UNRN. Consejo Nacional de Investigaciones Científicas y Tecnológicas (CONICET). Av. Roca, 1242, R8332EXZ General Roca, Río Negro, Argentina.

[5]Grupo Aragosaurus-IUCA, Facultad de Ciencias, Universidad de Zaragoza, C/ Pedro Cerbuna, 12, 50009 Zaragoza, Spain.

[6]Department of Humanistic Studies, Università CàFoscari Venezia, Dorsoduro 3484/D, 30123 Venezia, Italy. fbernard@ictp.it

[7]Multidisciplinary Laboratory, The Abdus Salam International Centre for Theoretical Physics, Strada Costiera, 11, 34151 Trieste, Italy.

*Corresponding author: pcruzado@ull.edu.es

Orcid:

Josep Fortuny**:** 0000-0003-4282-1619

Penélope Cruzado-Caballero: 0000-0002-5819-8254

Federico Bernardini: 0000-0002-3282-8799

Carolina Castillo Ruiz: 0000-0003-3381-7490

Abstract

An iconic, insular, endemic genus of lizards (*Gallotia*) is present on the Canary Islands (Spain), comprising gigantic to smaller-sized species. Despite numerous studies on various biological aspects of this genus, the osteological knowledge available is scarce. This makes it difficult to identify to species level the bone remains recovered from both living and extinct taxa, which is essential to understanding the evolution of this genus through time, its distribution and its migratory patterns. Herein, a detailed description, comparison and discussion of each mandibular bone of all the living giant species and the fossil taxon *G. goliath* is presented. First detailed descriptions of *G. intermedia* and *G. bravoana* are presented, and interspecific and ontogenetic characters to be considered for *Gallotia* and related taxa in future works are proposed. Disentangling the intra- and interspecific variability of the mandible, as well as its ontogenetic changes through time, is of special interest for a variety of reasons. These include: a) to evaluate paleobiodiversity; b) to evaluate intraspecific variation and ontogenetic changes; c) to establish mandibular characters for specific identification; d) as previous step in performing computational biomechanics studies based on 3D models to shed in-depth light on feeding ecology.

Key words: comparative morphology, ontogeny, paleoherpetology, Lacertidae, endemism, Canary Archipelago

Introduction

The Canary Archipelago has various endemic species, with the lizard genus *Gallotia* Boulenger, 1916, being its most iconic representative. This genus belongs to the family Lacertidae and includes four extant giant species (*Gallotia stehlini* Schenkel, 1901; *G. simonyi* (Steindachner, 1889); *G. intermedia* Hernández, Nogales and Martín, 2000; and *G. bravoana* (Hutterer, 1985)), two extinct giant species (*G. goliath* (Mertens, 1942) and *G. auaritae* Mateo, García Márquez, López Jurado and Barahona, 2001) and three extant smaller-sized species (*G. caesaris* (Lehs, 1914); *G. galloti* (Oudart, 1839); and *G. atlantica* (Peters and Doria, 1882)).

The fossil record of this genus goes back to the Pleistocene, except for *G. intermedia* and *G. simonyi*, which are recorded since the Holocene (Cruzado-Caballero et al., 2019; Palacios-García et al., 2021). Until the 1980s, living populations of giant species were historically believed only to contain the taxon *G. stehlini* on the island of Gran Canaria (López-Jurado, 1989). In the course of that decade, however, the first living populations of *G. simonyi* on the island of El Hierro were described, and a few years later, in 1996 and 1999, living individuals of *G. intermedia* and *G. bravoana* were described on the islands of Tenerife and La Gomera, respectively (Hernández et al., 2000; Nogales et al., 2001). All these species are in danger of extinction according to the IUCN ("critically endangered" in the case of *G. intermedia*, *G. bravoana* and *G. simonyi*; "least concern" in the case of *G. stehlini*), and all except *G. stehlini* are classified as "endangered" according to the Spanish Catalogue of Threatened Species (Spanish Royal Decree 139/2011). Only two of them currently have centers dedicated to the recovery of their populations (*G. simonyi* and *G. bravoana*). This is particularly dramatic given the appearance in recent times of the invasive North American snake *Lampropeltis getula californiae*, with increasing

populations of this predator (Friebohle, 2019; Piquet and López-Darias, 2021) as well as of domestic cats (Medina and Nogales, 2009).

The taxonomy of giant species has been based primarily on osteological characters in recent decades (Castillo et al., 1994; Barahona et al., 1998, 2000; López-Jurado, 1989; Hernandez et al., 2000; Nogales et al., 2001), but currently also incorporates molecular/genome analyses (Cox et al., 2010; Suárez et al., 2010; García-Porta et al., 2019). However, our current knowledge based only on morphological analyses is clearly limited and out of date, making it difficult or impossible to provide confident taxonomic determinations to species level and evaluate the intra- and interspecific variability of extant species. This is of the utmost importance in analyzing the taxonomy of extinct species known from several specimens recovered on the various islands of the Canary Archipelago, but for many years neglected (Cruzado-Caballero et al., 2019).

In this respect, mandibles are particularly important as they represent many diagnostic osteological characters of the species belonging to the genus *Gallotia* (Barahona et al., 1998, 2000; Palacios-García et al., 2021). They assume even greater importance in light of the fossil record, moreover, for mandibles are usually better preserved than crania, since the latter tend to disarticulate easily during the process of fossilization. On the other hand, the use of (micro-) computed tomography (CT) on biological and paleontological samples has increased greatly in recent years (e.g., Abel et al., 2012; Pandolfi et al., 2020), as this represents a useful tool for digitally exploring both inner and external morphology, paving the way to digitally extracting each bone and characterizing it in isolation, as well as obtaining high-resolution three-dimensional models and meshes. These models can also serve as a preliminary step for a variety of applications, such as 3D printers, computational

biomechanics, and 3D geometric morphometric studies (e.g., Marcé-Nogué et al., 2015; Pandolfi et al., 2020).

Taking into account the aforementioned considerations, the main goals of the present work are: 1) to provide detailed descriptions, based on micro-CT scanning, not only of each mandibular bone, but also of the four extant giant species and one fossil giant species of *Gallotia* as a whole; 2) to evaluate diagnostic characters for the different taxa; and 3) to start to collect the data required to identify intra- and interspecific variability and ontogenetic changes in the morphology of the mandible. Overall, we aim to shed light on the mandibular morphology of this endemic insular genus associated with its trend towards gigantism, seeing this as a previous step to future paleontological investigations and computational biomechanics analyses.

Material and methods

Institutional abbreviations.

CRLGH, Centro de Recuperación del Lagarto Gigante de El Hierro (El Hierro, Canary Islands, Spain); DZUL, Department of Zoology, University of La Laguna (Tenerife, Canary Islands, Spain); PCCRULL, Paleontology Collection-Carolina Castillo Ruiz, University of La Laguna (Tenerife, Canary Islands, Spain); TFMC-VT, Museum of Nature and Archaeology of Tenerife, terrestrial vertebrates (Tenerife, Canary Islands, Spain); UMCG, Environment Unit of the Island Council of La Gomera (La Gomera, Canary Islands, Spain); UMCIH, Environmental Unit of the Island Council of El Hierro (El Hierro, Canary Islands, Spain).

Material

This work is based on wet-prepared skeletons, except for the fossil taxon, because the species analyzed in the present study are classified as “ritically endangered” or “endangered” species, and wildlife rehabilitation centers do not exist for all the species, making it difficult to obtain specimens for their study. Six specimens were used: PCCRULL1195 (previously labelled H010 by Cruzado-Caballero et al., 2019), a fossil jaw of *Gallotia goliath* recovered from the island of El Hierro; PCCRULL1250 (previously labelled UMCG Gb01/2015 by Cruzado-Caballero et al., 2019), a subadult male individual of *Gallotia bravoana*; PCCRULL1251, a mature male individual of *Gallotia bravoana*; DZUL-2208, a mature male individual of *Gallotia intermedia*; CRLGH Gs-1/2015 (previously labelled UMAH Gs-1/2015 by Cruzado-Caballero et al., 2019), a mature male individual of *Gallotia simonyi*; TFMC-VT96, a mature male individual of *G. stehlini*. In the case of *G. bravoana*, except when specified, we refer by default to the adult specimen.

See Tables 1-3 for measurements.

Microtomography

All the specimens except the adult specimen of *G. bravoana* were scanned at the International Centre for Theoretical Physics (ICTP, Trieste, Italy), using an X-ray micro-CT scanner. For further details regarding the equipment see Tuniz et al. (2013). The micro-CT acquisitions of the specimens were carried out using a sealed X-ray source (Hamamatsu L8121-03) at a voltage of 110 kV, a current of 90 μA and with a focal spot size of 5 μm. The X-ray beam was filtered by a 1 mm-thick aluminum absorber. The resulting micro-CT slices were reconstructed using the commercial software DigiXCT (DIGISENS) in 32-bit format and obtaining a voxel size of 39.71 μm for all the specimens except for *G. goliath*,

which was scanned with a voxel size of 44.88 μm (see Cruzado-Caballero et al., 2019). The adult specimen of *G. bravoana* was scanned at the Centro Nacional de Investigación sobre Evolución Humana (CENIEH, Burgos, Spain), using a high-resolution x-ray tomography V|Tome|X s 240 micro-CT scanner (GE Sensing & Inspections Technologies). The specimen was scanned at 210 kV and 290 μA, obtaining a voxel size of 74.9 μm. Raw data from each scan were imported (as a stack of TIFF 8-bit files) to Avizo 7.0 to generate 3D models from the micro-CT images (similarly to Bolet et al., 2014; Cruzado-Caballero et al., 2019). A 3D model of each mandibular bone was generated for each specimen analyzed. The models of *G. goliath*, *G. intermedia* and *G. simonyi* correspond to the right mandible, whereas the models of both *G. bravoana* specimens and the *G. stehlini* specimen correspond to the left mandible. This is in accordance with the quality of the image in the X-rays, which in some cases were better able to visualize one side rather than its counterpart. For the purposes of visualization and comparison, the mandibles were mirrored where required.

Digital surface models of the studied mandibles and bones are available on MorphoSource (http: XXXX). All the models are available there upon request.

Requests for micro-CT raw data should be addressed to Josep Fortuny and/or Penélope Cruzado-Caballero.

Using the measurement tools provided by Avizo 7.0 software, the following measurements were carried out (Fig. 1): A) total anteroposterior length of the mandible, measured between the anterior ends of the dentary and the posterior of the articular; B) anteroposterior length of the subdental shelf, measured between the most proximal end of the dentary and the last tooth of the dentary; C) dorsoventral height of the mandible, measured from the apex of the coronoid to the ventral edge of the mandible; D) angle of the

coronoid, measured with respect to the axial plane of the mandible; E) angle of the posterior fossa of the coronoid, measured between the ridges of the posteromedial process of the coronoid.

The morphological description and anatomical nomenclature mainly follow Evans (2008), Rage and Augé (2010), Klembara et al. (2010, 2014), Gauthier et al. (2012), and Čerňanský et al. (2017).

Results

General remarks on the mandible

The mandible of the lizard genus *Gallotia* displays the typical shape also found in other lacertoid species (Figs. 1-2). This is composed of the following bones: dentary, splenial, coronoid, angular, surangular and articular. It also bears teeth. In lateral view, the general shape of the mandible is rectangular, with a markedly convex ventral border and a slightly concave dorsal border. In lateral view, there are several nutritional foramina distributed in a straight line, visible along the anterodorsal half of the dentary. In medial view, the anterior mylohyoid and anterior inferior alveolar foramina of the splenial, the posterior mylohyoid foramen of the angular, the mandibular fossa, and the surfaces of the retroarticular process and glenoid fossa are visible in all cases.

The two anteroposteriorly longest jaws among the extant species belong to *G. simonyi* and *G. stehlini*. These are approximately half the length of the extinct giant taxon *G. goliath* (Table 1; Fig. 2). The next-longest mandibles are clearly smaller: *G. bravoana* and the shortest, *G. intermedia* (Fig. 2; Table 1). The mandibular symphysis is flat, as in *Amphisbaena fuliginosa* (Gauthier et al., 2012). As regards the maximum dorsoventral height (between the ventral edge of the mandible and the dorsal edge of the coronoid; see

Figs. 1-2), the extant species *G. simonyi* has the greatest height, whereas *G. intermedia* has the least (Table 1). The greatest height found in living taxa is almost half that of *G. goliath* (24 mm, Table 1). In the following section, each mandibular bone is described in detail for each taxon analyzed.

Dentary

The dentary has a triangular shape with ventral borders that are convex in lateral view as in *Psammodromus*, Gallotiinae, Lacertinae and Varanoidea (Fig. 3; Gauthier et al., 2012; Čerňanský et al., 2016, 2017). The dentary is not strongly curved, and the anterior region is not very elevated dorsally, except in *G. simonyi* and *G. bravoana*, where the mandibular symphysis is higher than the mid-portion of the dental shelf (unlike in the rest of the species). As in other lacertids, anguids and scincids, the mandibular symphysis is narrow and almost horizontal (Villa and Delfino, 2019). The anterior end (symphysis area) of the dentary is slightly curved medially in dorsal view (Fig. 3). The dorsal border of the dentary varies from straight in the subadult *G. bravoana* to slightly concave in *G. goliath*, *G. intermedia* and *G. stehlini* and strongly concave in *G. simonyi* and in the adult *G. bravoana* (Fig. 3), in lateral view.

The anteroposteriorly longest dentary among the extant species corresponds to *G. stehlini* and *G. simonyi*, but these are half the length of that of the fossil taxon *G. goliath* (Table 1). In comparison, this length in *G. intermedia* and *G. bravoana* is one third that in *G. goliath* (Table 2). This bone is slightly longer (54-57% of the total length of the mandible; Tables 1-3) than the length of the postdentary section of the mandible (surangular, angular and articular) in all the studied specimens, as in the members of Lacertinae except for *Psammodromus* and *Dracaenosaurus*, where they are equal in length (Čerňanský et al.,

2016, 2017). This bone posteriorly overlaps the postdentary bones laterally, in a reduced form as in the clade Varanoidea (Gauthier et al., 2012). The transverse section is C-shaped, being less pronounced in the fossil taxon *G. goliath* and the extant taxon *G. bravoana* than in the rest of the species in posterior view.

In close-up of theanterior view, the micro-CT scan of the mandible shows the dentary to be suspended from the coronoid, surangular, splenial and angular, as in the iguanid *Morunasaurus annularis* (Gauthier et al., 2012). The external surface is pierced by a variable number of oval-shaped labial foramina (Figs. 2-3; Table 1). These are distributed in a straight line along the midline of the dentary. *G. intermedia* has five labial foramina, whereas *G. goliath* and *G. bravoana* have seven labial foramina, and in the subadult *G. bravoana* there are six (Tables 1 and 4). These labial foramina are similar in size, as occurs in the rest of the species of the clade Gallotiinae (Čerňanský et al., 2016, 2017). In contrast, the labial foramina of *G. simonyi*, of which there are seven, increase in size backwards, whereas in *G. stehlini* the last labial foramen is larger than the rest, similarly to the anguimorphid *Lanthanotus borneensis* (Gauthier et al., 2012). This confirms the variation in number and distribution of the foramina previously observed by Barahona (1996) in *G. galloti* with 5-7 labial foramina in a straight line, but it also reveals a variation in the size of the labial foramina. Through these labial foramina pass the endings of the inferior alveolar nerve corresponding to the cutaneous branch of the mandibular nerve (Oelrich, 1956; Barahona, 1998).

In adults of the genus *Gallotia*, the posterodorsal (coronoid) process is anteroposteriorly longer than the posteroventral (angular) process, as in Anguidae but unlike in Agamidae, *Algyroides*, *Anatololacerta*, *Dalmatolacerta*, *Lacerta*, *Podarcis*, *Psammodromus*, *Timon*, *Zootoca* and Scincidae, among others (Barahona, 1996; Barahona and Barbadillo, 1998;

Čerňanský et al., 2016, 2020; Villa and Delfino, 2019; Čerňanský and Syromyatnikova, 2021). This feature can be observed in *G. goliath*, *G. intermedia* and *G. stehlini*, whereas in *G. bravoana* and in *G. simonyi* the two processes are similar in length in the adult (and in the subadult *G. bravoana*) (Table 4). In lateral view, the posterodorsal (coronoid) process is shorter, not reaching the height of the apex of the coronoid, in all the species except *G. intermedia*, in which this process subsequently surpasses the apex of the coronoid, as in the iguanid *Dipsosaurus dorsalis* (Gauthier et al., 2012). In a close-up anterior cutaway view of the mandible, it lies flat against the dorsolateral face of the surangular below the coronoid, as in the xenosaurid *Xenosaurus grandis* (Gauthier et al., 2012). The end of the posteroventral process is located approximately at the height of the coronoid apex in *G. goliath*, *G. bravoana* and *G. intermedia*, whereas in the other species and in the subadult *G. bravoana* the posteroventral process ends before the anterior border of the coronoid. Although this can be slightly variable, especially in subadults and among other lacertids, this character is only observed in the lacertid *Acanthodactylus* and differs from what is seen in *Psammodromus*, *Dalmatolacerta*, *Anatololacerta*, *Timon*, *Podarcis* and *Zootoca*, where the posteroventral process extends as far as or beyond the apex of the coronoid (Čerňanský et al., 2016). These processes are separated by a wedge-shaped anterior extension of the surangular and angular bones in lateral view, which approaches the anterior end of the anterolateral coronoid process. In *G. goliath*, the subadult *G. bravoana* and *G. intermedia*, the anterior end of the extension is sharper, whereas in *G. stehlini* it is straight. In *G. simonyi* and the adult *G. bravoana* there is a forked end to the surangular due to one or two filiform projections, respectively.

The medial side of the dentary is concave and presents a dental (or subdental) shelf (Table 1). The dental shelf is dorsoventrally wide, and it sharpens posteriorly in medial view.

Based on the micro-CT scans (see slices in Supplementary Information), it can be observed that this shelf is weakly developed in the anterior part of the dentary, as in the clades Gymnophthalmidae, Anguidae and Varanoidea and in fossorial forms (Gauthier et al., 2012). The dental shelf lies between the alveolar shelf (situated dorsally) and the Meckelian canal (situated ventrally) and does not present the hooks around the anterior rim of the anterior inferior alveolar foramen, as in the case of the lacertid *Celestus enneagrammus* (Gauthier et al., 2012). The Meckelian canal is deeply excavated, anteriorly narrow, posteriorly wide, and open medially along its entire length. The lower dentary border of the Meckelian canal folds up so it closely approaches the upper border, restricting the canal as in the clade Hoplocercinae (Gauthier et al., 2012).

Splenial

This is a long, flat and inverted-diamond-shaped bone that covers the Meckelian canal attachment to the dentary above the canal, as in lacertids and anguids (Villa and Delfino, 2019; Fig. 4). This bone overlaps the angular, as can be observed in the micro-CT scan (see slices in Supplementary Information), as in the iguanid *Crotaphytus collaris* (Gauthier et al., 2012).

The profile of the dentary is like that present in lacertoids, triangular with a concave dorsal border and a convex ventral border, unlike what is present in Scincidae (Villa and Delfino, 2019). The anterior end of the ventral border of *G. goliath* is narrow and dorsally markedly elevated. The anteroposteriorly longest splenial among the extant species corresponds to *G. simonyi*, being approximately half the length of that of *G. goliath*. The shortest is *G. intermedia* (Fig. 4; Table 2). In extant species, the length of this bone is 45-48% of the total length of the mandible, whereas in *G. goliath* it is 55.2% (Table 3). The anterior length is

almost three-quarters the length of the dentary tooth row, as in the clades Priscagaminae, Polyglyphanodontia, Scleroglossa, Tupinambinae, Xenosauridae, Gerrhonotinae, Diploglossinae and Pan-Varanoidea and in fossorial forms (Gauthier et al., 2012). The distal end is wedge-shaped and enters between the surangular and angular. In *G. stehlini* this posterior part reaches as far as the anterior border of the dorsal process of the coronoid in medial view. In the rest of the specimens, it extends to the apex of the dorsal process of the coronoid, similar to the gallotiinids *Pseudeumeces* and *Dracaenosaurus* (Augé and Hervet, 2009; Čerňanský et al., 2017).

The anterior mylohyoid and the anterior inferior alveolar foramina are located around the middle of the bone, as in the lacertids and unlike in Scincidae (Villa and Delfino, 2019). The anterior mylohyoid foramen has an ellipsoidal shape and is located in the dorsal half of the bone near the dorsal border. This foramen is located between the 13th and the 22nd tooth positions (counting from anterior to posterior; Table 1), with the most anterior position found in *G. bravoana* (13th) and the most posterior position in *G. goliath* (22nd). The location of the anterior mylohyoidin relation to the mylohyoid foramen is anterodorsal in all specimens, as in *Spathorhynchus fossorium* and *Dyticonastis rensbergeri* (Gauthier et al., 2012). Below the anterior mylohyoid foramen is the anterior inferior alveolar foramen, which is partially open in lateral view in *G. bravoana* (subadult) and *G. intermedia*, completely open in *G. goliath*, *G. stehlini* and *G. simonyi*, but closed in the adult *G. bravoana*. In the latter taxon, there is a second small foramen located anteroventrally to the anterior mylohyoid foramen. Both foramina are traversed by the inferior alveolar nerve (Oelrich, 1956; Barahona, 1996). It should be noted that the fossil taxon *G. goliath* has three foramina, two located anteroventrally and one posteroventrally to the anterior mylohyoid foramen.

Coronoid

The coronoid is a bone of an inverted chevron shape, which labially overlaps the dentary, as in lacertids (Gauthier et al., 2012; Villa and Delfino, 2019; Fig. 5). The anteroposteriorly longest coronoid corresponds to *G. goliath*, followed by *G. stehlini* (Table 2). In extant species, the length of this bone is 27-34% the total length of the mandible, in clear contrast with the extinct taxon *G. goliath*, where it is 23.8% (Table 3). The coronoid is composed of four processes: anterolateral, anteromedial, posteromedial and dorsal. The dorsal process has a rounded dorsal end and forms an approximate right angle with respect to the axial plane of the mandible in *G. intermedia*, *G. simonyi*, *G. bravoana* and *G. stehlini* (Fig. 1-2; Table 4). In *Acanthodactylus erythrurus*, *Algyroides fitzingeri*, *Algyroides marchi*, *Ophisops elegans*, *G. goliath* (present study) and in juveniles of other species (Villa and Delfino, 2019), as in the subadult *G. bravoana* (present study), this process is slightly posteriorly directed (approximate angle of 70º in *G. goliath* and *G. bravoana*; see Table 4 for *Gallotia* specimens and Villa and Delfino, 2019 for other taxa). The process is robust in *G. goliath*, *G. simonyi*, *G. bravoana* and *G. stehlini* and anteroposteriorly narrow in the subadult *G. bravoana* and *G. intermedia*. In lateral view, the process has a ventrodorsally developed sloping ridge, followed posteriorly by a concave zone associated with the insertion of the external adductor (M. *adductor mandibulae externus superficialis*), which continues in the dorsal part of the surangular and suggests a prominent development of this musculature (Augé and Hervet, 2009; Čerňanský et al., 2017). This concave area is wide and shallow in all the taxa except for the subadult *G. bravoana*, where it is deeper and narrower.

The anterolateral and anteromedial processes overlap the posterior end of the dentary, laterally and medially respectively. The micro-CT scan reveals that the anteromedial process fits into the sulcus beneath the tooth-bearing border of the dentary (see slices in Supplementary Information), as in the clades Priscagaminae, Acrodonta, Iguaninae, Polyglyphanodontia, Scleroglossa, Lacertoidea, Globauridae, Scincidae, Xenosauridae, Glyptosaurinae and Rhineuridae (Gauthier et al., 2012). In the clade Squamata, micro-CT scans also show that the coronoid arches above the dorsal margin of the mandible to reach the lateral face of the surangular (Gauthier et al., 2012, and see slices in Supplementary Information). The angle between the anteromedial and posteromedial processes in the genus *Gallotia* is most acute within the clade Gallotiinae (Čerňanský et al., 2016, 2017). Whereas in *Dracaenosaurus* and *Janosikia* the angle is around 75º-80º (Čerňanský et al., 2016, 2017), in *G. stehlini* it is 66°, and in the rest of the extant and fossil specimens it is between 44° and 51°. *G. bravoana* and *G. stehlini* present a very short anterolateral process reaching the last tooth position of the dentary, but not as short as in *Dracaenosaurus*, where it does not reach the dental battery (Čerňanský et al., 2017). In contrast, this process in *G. intermedia* and *G. goliath* surpasses the penultimate and in *G. simonyi* the antepenultimate tooth position, respectively. In *G. goliath*, the subadult *G. bravoana*, *G. intermedia* and *G. simonyi*, this process is triangular in shape in lateral view, as in *G. galloti* and *Dracaeonosaurus* (Barahona, 1996; Čerňanský et al., 2017), but unlike *G. stehlini* and *G. bravoana*, where it is rectangular in shape.

In medial view, the anteromedial process has a triangular or wedge shape, as in *G. galloti* and *Dracaenosaurus* (Barahona, 1996; Čerňanský et al., 2017). In the subadult *G. bravoana*, *G. intermedia* and *G. stehlini*, the anterior extension of this process reaches the last dentary tooth, whereas in *G. goliath*, *G. bravoana*, and *G. simonyi* it reaches the antepenultimate

tooth, unlike in *Dracaenosaurus*, where it does not reach the dental battery (Čerňanský et al., 2017). In this medial view, the posteromedial process is rectangular, except in the subadult *G. bravoana*, where it has a pointed ventral margin. The posterior border of this process has a sigmoid shape similar to that of *G. galloti*, but it is more marked in all the species except for *G. goliath*, *G. bravoana* and *G. intermedia*, where it is concave (Barahona, 1996). In *G. bravoana* (very shallow), *G. intermedia* and *G. simonyi*, this posteromedial process has an additional posterior S-shaped ridge (Fig. 5). The medial surface of this process is concave (in contact with the anterior margin of the adductor fossa) and deep in all the adult specimens but shallow in the subadult *G. bravoana*. It presents an anterior marked coronoid ridge in all the taxa (Fig. 5; Table 4).

Angular

The angular is anteroposteriorly elongated and dorsoventrally flattened, with the anterior end narrower than the posterior end, and it presents a concave dorsal border and a convex ventral border (Fig. 6). As in other lacertids, the medial exposure of this bone is reduced and it is broadly separated from the coronoid (Gauthier et al., 2012). This bone is responsible for the form of most of the floor of the adductor (mandibular) fossa. The anteroposteriorly longest angular among the extant species corresponds to *G. simonyi* (being approximately half the length of that of *G. goliath*), whereas the shortest is *G. intermedia* (Table 2). The length of this bone is 55-62% of the total length of the mandible, whereas it is 50% in *G. goliath* (Table 3). The angular articulates with the dentary through a shark-fin-shaped articulation facet located on its lateral side and with the posterior end of the splenial through the angular ridge on the medial side (Fig. 6 B, D, F, H, J and L). The posterior end is triangle-shaped in all extant species, with the dorsal side longer than the ventral side in lateral view. In *G. goliath*

this bone is barely exposed laterally. In *G. goliath* and the subadult *G. bravoana*, the posterior edge reaches the posterior external foramen of the surangular, whereas in the other species it ends earlier.

In medial view, the posterior mylohyoid foramen of the angular is located below the apex of the coronoid in *G. goliath*, *G. intermedia*, *G. bravoana* and *G. simonyi*, as in the gallotiinids *Dracaenosaurus* and *Pseudeumeces*, *Tepexisaurus tepexii* and Xantusiidae, and anterior to the apex in *G. stehlini*, as in the clades Varanoidea and Serpentes (Augé and Hervet, 2009; Gauthier et al., 2012; Čerňanský et al., 2017).

Surangular

The surangular is an anteroposteriorly elongated bone with a rectangular morphology whose length in extant species is 55-62% the length of the mandible, whereas in *G. goliath* it is 47.7% (Fig. 7; Table 3). This bone forms the posterodorsal border of the mandible. Among the specimens studied, the longest one anteroposteriorly is that of *G. simonyi*, whereas the *G. intermedia* specimen is the shortest (Table 2). The dorsal margin is nearly horizontal, rising slightly toward the coronoid, with the anterodorsal edge set below the level of the tooth crowns, as in the anguimorphid *Lanthanotus borneensis* (Gauthier et al., 2012). The posterior end of the surangular is fused with the articular only in *G. intermedia* and *G. simonyi*, as previously described by Barahona (1996), who found that the articular and surangular bones are fused in adult individuals of *G. galloti*. This is partially coincident with adult lacertids, where the surangular and articular are fused with the prearticular (Villa and Delfino, 2019).

In lateral view, the surface of this bone has a slight dorsal longitudinal depression with a ridge separating the ventral half. This occurs in all specimens except in the subadult *G. bravoana*, where the dorsal surface is slightly convex (Table 4). The dorsal depression of the

surangular, together with the posterior part of the dorsal process of the coronoid, forms the insertion area of the M. *adductor mandibulae externus superficialis* (Barahona, 1996). A micro-CT scan shows that in the dorsolateral face of the adductor (mandibular) fossa, the lateral wall is below the medial wall, as in Tropidophiidae and Caenophidia (Gauthier et al., 2012). This fossa in lateral view is shallow and extends ventrally no more than halfway down, as in the clades Cordylidae and Carusiidae (Gauthier et al., 2012).

In the lateral surface of the dorsal area there are two foramina, one anterior and one posterior, which communicate with the mandibular fossa in medial view, as in the scincid *Brachymeles gracilis* (Gauthier et al., 2012). Both foramina are associated with the transmission of the cutaneous branches of the inferior alveolar nerve (Barahona, 1996). The anterior foramen is larger than the posterior one in all specimens except in *G. intermedia*, where they are of similar size. On the other hand, *G. simonyi* has a third foramen in the ventral half of the surangular. The extinct taxon *G. goliath* also has a third foramen present in the ventral border near the posterior end of the bone.

In medial view, a large part of the adductor (mandibular) fossa is visible. This fossa is mostly formed by the surangular, except for small ventral and anterior parts that belong to the articular and angular, respectively. In the anterior half of the dorsal border of the adductor (mandibular) fossa, the articulating facet of the coronoid is ellipsoidal in shape. This ellipsoidal shape is narrower dorsomedially in the subadult *G. bravoana* and wider in the rest of the specimens, with the maximum width found in *G. stehlini*. Posteriorly, the surangular is forms part of the glenoid fossa together with the articular, where the mandible articulates with the skull.

Articular

This bone is in contact with the coronoid, the surangular and the angular in the posterior section of the mandible (Fig. 8). It is an anteroposteriorly elongated bone (59-65.5% of the length of the mandible; Table 3), with a subrectangular shape in medial view. In this view, it can be observed that the anterior and posterior ends are sharpened, the posterior end being the thicker of the two. The longest articular among the extant species corresponds to *G. stehlini*, whereas the shortest belongs to *G. intermedia* (Table 2).

In dorsal view, in *G. goliath* the medial side is straight, and the lateral side is convex, whereas in the extant species the medial side is concave, and the lateral side is convex. Thanks to the isolated 3D model of each mandibular bone, it can be seen that the articular has a deep and marked groove on its medial side that extends almost the entire length of the bone and anteriorly finishes on a sharp splenial process (Fig. 8). The groove is broader lateromedially in *G. goliath* and *G. simonyi* than in the rest of the species.

In medial view, the dorsal border of the anterior and posterior sections is straight and is anteroventrally or posteroventrally directed, respectively. This border is markedly concave at the half section, whereas the ventral border is almost straight, with the posterior end dorsally directed in all the specimens except in the subadult *G. bravoana*, where it is ventrally directed. Another exception is *G. stehlini*, where it is straight.

The medial side of this bone forms the ventral border of the adductor (mandibular) fossa. The facet to the articulation with the coronoid located on the lateral side is tongue-shaped in all species except in *G. bravoana* and *G. simonyi*, where it is arrowhead-shaped as in *G. galloti* (Barahona, 1996).

In medial view, there are two articulation facets to the dentary and the coronoid. Both facets are arrow-shaped. The dentary facet is the longer anteroposteriorly whereas the coronoid facet, located posterodorsally to the former, is slightly higher dorsoventrally.

In the posterior section, the glenoid fossa, the retroarticular process and the tympanic ridge are located. The first is dorsal, articulates with the quadrate, and is deeper in *G. goliath, G. simonyi* and *G. intermedia* than in *G. bravoana* and *G. stehlini*. The second is on the ventral side and is almost equal to or slightly narrower than the glenoid in all species, forming a pyramid-shaped process, as is also the case in many lacertid lizards (Augé and Hevert, 2009). Its dorsal surface is inclined posterodorsally in lateral view, as in the clade Agaminae (Gauthier et al., 2012). In dorsal view, it can be seen that the retroarticular process is not inflected medially in *G. simonyi* and *G. stehlini*, unlike in *G. goliath, G. bravoana*, *G. intermedia* and the clades Cordylidae and Anguidae and absent of the lateral notch as in *Uranoscodon superciliosus* (Gauthier et al., 2012). In lateral view, this process is longest in the subadult *G. bravoana*, whereas it is shortest and least developed in *G. simonyi*. The posterior end of this process is markedly inclined ventrally in the subadult *G. bravoana*; it runs in a straight line in *G. intermedia* and *G. stehlini*; and it is dorsally inclined in *G. goliath*, the adult *G. bravoana* and *G. simonyi*, as well as in the gallotiinids *Pseudeumeces* and *Dracaenosaurus* (Augé and Hevert, 2009; Čerňanský et al., 2017). The foramen for the chorda tympani is located on the dorsal surface. Together with this foramen, there are other accessory foramina, one in *G. simonyi* and two in *G. stehlini*. The tympanic ridge can be seen to be anteroposteriorly directed in medial view under the glenoid fossa and the retroarticular process. This is relatively shorter in *G. simonyi* than in the rest of the specimens and is straight in all the species except *G. simonyi*, where it is sigmoidal.

Dentition

The dentition in all the mandibles is pleurodont and heterodont with respect to the shape of the proximal section of the tooth and the number of cusps (Fig. 2). The teeth are conical, with a width that increases posteriorly, as in the clade Gallotiinae (Augé and Hevert, 2009; Čerňanský et al., 2016, 2017). According to Čerňanský et al. (2016, 2017), robust teeth and a low tooth count are shared with members of the clade Gallotiinae, especially the genus *Gallotia*.

The number of tooth positions is variable across the sample analyzed: the maximum number is found in *G. goliath* (32), followed by *G. stehlini* (26), *G. intermedia* (25) and *G. simonyi* (23), despite the latter having the greatest length, whereas the lowest number is found in *G. bravoana* (21) (Table 1). It should be noted that this number increases with the size of the individual (Table 1; Barahona et al., 2000). According to Čerňanský et al. (2016), the low dentary tooth count is shared with members of the clade Gallotiinae, whereas most members of the clade Lacertinae have a higher tooth count with more slender teeth (Čerňanský et al., 2016). The number of dentary teeth per millimeter of the dental shelf falls between a maximum of 1.3 in *G. intermedia*, followed by the adult *G. bravoana* with 1.1 and *G. simonyi* with 0.9, whereas the minimum is found in *G. goliath* with 0.6 (Table 1).

The members of the clade Gallotiinae *Janosikia*, *Dracaenosaurus* and *Pseudeumeces* present unicuspid teeth with a blunt cylindrical form, unlike the multicuspid teeth (between two and five cusps) present in the genus *Gallotia* (Augé and Hevert, 2009; Čerňanský et al., 2016, 2017). In the genus *Gallotia*, the first dental positions are occupied by monocuspid teeth, asymmetric in lingual view and with the cusp oriented distally. The intermediate positions are occupied by larger teeth, with a distal main cusp and probably a much smaller mesial cusp or a tricuspid form, in the latter case the central cusp being the main one and

the mesial and distal ones secondary, as in *G. galloti* (Barahona, 1996). In some cases, the posterior positions present tricuspid teeth, as in *G. bravoana* (subadult) and *G. intermedia*. Moreover, ontogenetic change has been observed in the tooth morphology of extant lacertids, as in *G. stehlini*, where juvenile tricuspid teeth are replaced by multicuspid teeth in the adult (Barahona et al., 2000). However, in the case of *G. simonyi* the number of cusps is constant during ontogeny except in some large individuals, in which an additional anterior or posterior cusp may appear (Barahona et al., 2000).

Discussion

Review of previously analyzed characters

Comparative analysis of the general mandibular morphology reveals a considerable reduction in total size between the extinct taxon (*G. goliath*) and the extant taxa, ranging from a minimum of 48.7 - 49.1% (*G. simonyi* and *G. stehlini* respectively) to a maximum close to 64.1% (*G. intermedia*). This reduction is reflected in most of the length and height measurements taken on the mandible as a whole, but also in each bone (Fig. 2; Tables 1-2). Furthermore, the number and location of mandibular foramina was a character first reported by Barahona et al. (1996), showing intraspecific and ontogenetic plasticity. However, the present study reveals that this character is also an interspecific signal within the genus *Gallotia* (see splenial bone; Table 4). At the same time, this study also reveals that not all the adult specimens of the fossil and extant taxa of the clade Gallotiinae have the following in common: a) a dentary that is poorly curved with an anterior region slightly elevated dorsally, and b) a symphysial area located slightly more dorsally than the middle part of the dental shelf. The studied *G. simonyi* specimen shows the opposite condition of these two characters, similarly to *Dracaenosaurus*, *Lacerta*, *Timon*, *Zootoca*, *Podarcis* and

Acanthodactylus, as the anterior region is strongly curved and dorsally elevated (Čerňanský et al., 2017).

Based on individual dentary bones, Barahona (1996) and Čerňanský et al. (2016) argued that in adult specimens (Table 4), the posteroventral process is generally shorter than the posterodorsal process of the dentary, which does not extend posteriorly beyond the apex of the dorsal process of the coronoid. Nonetheless, *G. bravoana* (subadult and adult) and *G. simonyi* are an exception to this pattern in that these processes are similar in size (Table 4). Barahona (1996) also reported that the surangular and articular bones are fused in adult individuals in the small-sized lizard *G. galloti*, suggesting that this could be a character with ontogenetic variation. However, in the studied adult specimens of *G. stehlini* and *G. bravoana* this fusion is not observed, and these bones are well defined along their entire length according to the X-ray tomographic slices. *G. simonyi* and *G. intermedia* present fused bones at the posterior end.

Analysis of the tomographic images shows attenuated or dark areas indicating a decrease in density of the bone tissue (Carrera et al., 2008). These areas are located in the posterior part of the surangular bone in the *G. simonyi* specimen, and in the posterior part of the joint around the glenoid fossa in *G. simonyi*, *G. stehlini* and the subadult *G. bravoana* specimen. These changes and differences in bone tissue densities and bone fusions among the *Gallotia* species may be associated with differences in longevity and time to sexual maturity, which may allow more prolonged growth, but not with differences in growth rates (Castanet and Baez, 1991), as reptiles continue growing after reaching full maturity (Kozlowski, 1996). All in all, it should be borne in mind that there are probably different growth rates among living and extinct species in inverse proportion to the size of the species; that is, smaller

taxa (such as *G. atlantica*) show a higher rate, whereas larger taxa display a lower growth rate (*G. goliath*; Castanet and Baez, 1991). On the other hand, the study of cranial osteology and its inter- and intraspecific variation carried out by Barahona (1996) and Barahona and Barbadillo (1998) on 13 species of lacertids from the Iberian Peninsula and the Canary species *G. galloti* showed: a) that the articular areas of the mandible undergo progressive ossification during ontogeny, leaving connective tissue types in the area of articulation between the mandible and the quadrate; b) that the retroarticular process of the articular and the posterior part of the surangular are completely ossified in adults. Finally, Barahona et al. (2000) observed that the giant species *G. stehlini* and *G. simonyi* show several characteristics acquired by pedomorphosis that are necessary to allow continuous growth and reach larger sizes. These characteristics include the lack or delay of ossification in the posterior aspect of the surangular and the weak development of the retroarticular process of the articular. The observations based on the present micro-CT scans of the *G. stehlini* and *G. simonyi* specimens thus confirm the results obtained by Barahona et al. (2000). Except for the fusion of the surangular and the articular bones, moreover, the results obtained for the subadult and adult *G. bravoana* partially agree with the results of Barahona (1996) and Barahona and Barbadillo (1998) for *G. galloti*.

Interspecific variation

During our analysis of the jaws under study, the following interspecific characters were detected (excluding the jaw of the subadult *G. bravoana*; Table 5): a) the location of the end of the posterodorsal process of the dentary (*G. intermedia* is the only species in which this process posteriorly surpasses the apex of the coronoid); b) the shape of the end of the

posterodorsal process of the dentary, with the presence/absence of small projections (one dorsal projection being present in *G. goliath*, one dorsal projection and one ventral projection in *G. simonyi* and *G. bravoana*); c) the shape of the posterior border of the posteromedial process of the coronoid (concave in *G. goliath*, *G. bravoana* and *G. intermedia*, and S-shaped in *G. stehlini* and *G. simonyi*); d) the presence/absence of an S-shaped dorsoventral crest on the posteromedial process of the coronoid (present in the jaws of *G. intermedia*, *G. bravoana* and *G. simonyi*, absent in *G. goliath* and *G. stehlini*); e) the degree of opening of the anterior inferior alveolar foramen of the splenial (completely open in *G. goliath*, *G. stehlini* and *G. simonyi*, partially open in *G. intermedia*, and closed in the adult *G. bravoana*); f) the degree of fusion of the surangular and the articular (not fused in *G. bravoana* and *G. stehlini*, partially fused in *G. intermedia* and *G. simonyi*); g) the direction of the retroarticular process of the articular with respect to the ventral border of the surangular (in a straight line in *G. intermedia* and *G. stehlini* and dorsal in *G. goliath*, *G. bravoana* and *G. simonyi*); and h) the degree of curvature of the jaw with respect to the axial plane (more pronounced in the jaw of *G. goliath*, *G. simonyi* and *G. bravoana*, intermediate in *G. intermedia* and *G. stehlini*).

Ontogeny in giant lacertids: Gallotia bravoana *as a case study*

The mandible of the subadult specimen of *G. bravoana* is nearly three quarters of the length of the adult *G. bravoana* and the *G. intermedia* specimens, half that of the *G. simonyi* and *G. stehlini* specimens (Fig. 2; Table 1), and a quarter that of *G. goliath*. It should be noted that some of the osteological features found in the subadult *G. bravoana* mandible were considered by Barahona (1996) and Čerňanský et al. (2016) to be typical of juvenile or subadult individuals, such as the small and posteriorly inclined dorsal process of the

coronoid (which in the adult is approximately at a right angle) or the short and poorly developed anteromedial process of the coronoid (more developed in the adult; Table 4). Both these traits confirm the subadult status of the *G. bravoana* specimen. However, two of the characters with an ontogenetic signal are open to debate. Firstly, according to Barahona (1996), in adult specimens of *G. galloti* Oudart, 1839, the posterodorsal process of the dentary is anteroposteriorly longer than the posteroventral process, whereas in juveniles the converse is the case. Yet the specimens of *G. bravoana* (subadult and adult) and *G. simonyi* (adult) studied herein both present posterodorsal and posteroventral processes with very similar lengths (Table 4). Secondly, the posterior inclination of the dorsal process of the coronoid is another debatable character because in *G. goliath* this process presents a posterior inclination similar to the subadult *G. bravoana*. Further subadult and juvenile specimens from all living species are required to ascertain whether these characters are useful for distinguishing between juveniles, subadults and adults.

Last but not least, analysis of the subadult *G. bravoana* specimen reveals potential additional characters that could be characteristic of a previously overlooked juvenile or subadult ontogenetic stage: 1) a shallow adductor fossa of the coronoid; and 2) the absence of the dorsal depression in the surangular in lateral view. It lies beyond the scope of the present study to test the implications of these characters in an ontogenetic framework. However, it would be of great interest for future research, calling for an analysis of a greater number of specimens from different taxa at different stages of development.

Conclusions

In addition to the size differences present in the analyzed taxa, some interspecific changes have been observed through the mandibles of giant members of the genus *Gallotia*. These changes can be summarized as relating to: a) the general morphology of the mandible with respect to its curvature; b) the degree of bone fusion of the surangular and articular; c) the presence of accessory projections in the posterodorsal (coronoid) process of the dentary; d) the degree of opening of the anterior inferior alveolar foramen of the splenial; e) variability in the morphology of the posteromedial process of the coronoid; and f) the degree of ventral inclination of the retroarticular process. Additionally, it has been observed that some changes that were thought to be due only to intraspecific and ontogenetic variations may instead represent interspecific variation, such as the number and distribution of the nutritional foramina and the location of the end of the posterodorsal (coronoid) process of the dentary. Finally, we tested ontogenetic variations in the length of the posterodorsal and posteroventral processes of the dentary (in the subadult and adult *G. bravoana* and in *G. simonyi* the two processes being found to be similar in length) and in the inclination of the dorsal process of the coronoid (inclined in *G. goliath*). All in all, these new results and osteological characters might prove helpful in identifying mandibular bones to species level. Nonetheless, future research is required to shed a more in-depth light on the ontogenetic signal found in different characters, and this requires further analysis of juvenile and subadult specimens in extinct and extant species. Notably, the 3D models used in the present study and the characters examined represent a preliminary step in performing the computational biomechanics analyses necessary for assessing the potential role of the variations observed and evaluating their potential functional signal.

Acknowledgements

We thank the Cabildo Insular of El Hierro and of La Gomera for access to specimens, and in particular Miguel Angel Rodríguez of the Unidad de Medioambiente del Cabildo Insular de El Hierro and Sonia Plasencia of the Unidad de Medioambiente del Cabildo Insular de la Gomera (Canary Islands, Spain), the Museum of Nature and Archaeology of Tenerife (Tenerife, Canary Islands, Spain), and Guillermo Delgado Castro, curator of the vertebrate collection. The micro-CT scanning of adult *G. bravoana* was performed at the CENIEH (Burgos, Spain) facilities with the collaboration of the CENIEH staff. Our special thanks go to Alex Serrano (ICP) for his help on the segmentation of this specimen. We acknowledge Dr. Andrej Čerňanský (Faculty of Natural Sciences, Department of Ecology, Comenius University in Bratislava, Bratislava, Slovakia) and Dr. Torsten M. Scheyer (Palaeontological Institute and Museum, University of Zürich, Zürich, Switzerland) for their valuable comments and suggestions, which have greatly improved the manuscript. This research has received support through the grants PROID1017010136 (C.C.R., P.C-C., J.F.), FCT-17-12775 (C.C.R., P.C.-C.), PID2020-117118GB-I00 funded by MCIN/AEI/ 10.13039/501100011033 (J.F. and C.C.R) and PID2020-114982RA-I00 funded by the University of La Laguna and the Spanish Ministry of Science, Innovation and Universities. (P.C-C. and C.C.R.). J.F. is a member of the consolidated research group (GRC) 2017 SGR 86. J.F. acknowledges support from the CERCA programme (ICP) of the Generalitat de Catalunya. Rupert Glasgow revised the text in English.

References

Abel, R.L., Laurini, C.R., Richter, M. 2012. A palaeobiologist's guide to 'virtual' micro-CT preparation. Palaeontol. Electron. 15, 2;6T,17

Augé, M.L., Hervet, S. 2009. Fossil lizards from the locality of Gannat (late Oligocene–early Miocene, France) and a revision of the genus *Pseudeumeces* (Squamata, Lacertidae). Palaeobiodivers Palaeoenviron 89(3-4):191.

Barahona, F. 1996. Osteología craneal de lacértidos de la Península Ibérica e Islas Canarias: análisis sistemático filogenético. (Doctoral dissertation, Universidad Autónoma de Madrid).

Barahona, F., Barbadillo, L.J. 1998. Inter-and intraspecific variation in the post-natal skull of some lacertid lizards. J. Zool. 245 (4):393e405.

Barahona, F., López-Jurado, L.F., Mateo, J.A. 1998. Estudio anatómico del esqueleto en el género Gallotia (Squamata: Lacertidae). Rev. Esp. Herp. 12:69-89.

Barahona, F., Evans, S.E., Mateo, J.A., García-Márquez, M., López-Jurado, L.F. 2000. Endemism, gigantism and extinction in island lizards: the genus *Gallotia* on the Canary Islands. J. Zool. 250(3):373-388.

Bolet, A., Delfino, M., Fortuny, J., Almecija, S., Robles, J.M., Alba, D.M. 2014. An amphisbaenian skull from the European Miocene and the evolution of Mediterranean worm lizards. PLoS One 9(6):e98082.

Boulenger, G.A. 1916. On the lizards allied to *Lacerta muralis* with an account of *Lacerta agilis* and *Lacerta parva*. Trans. R. Zool. Soc. Lond. 21(1):1e104.

Carrera, I., Hammond, G.J., Sullivan, M. 2008. Computed tomographic features of incomplete ossification of the canine humeral condyle. Vet. Surg. 37(3):226-231.

Castanet, J., Baez, M. 1991. Adaptation and evolution in *Gallotia* lizards from the Canary Islands: age, growth, maturity and longevity. Amphib-Reptil 12(1):81-102.

Castillo, C., Rando, J.C., Zamora, J.F. 1994. Discovery of mummified extinct giant lizards (*Gallotia goliath*, Lacertidae) in Tenerife, Canary Islands. Bonn. Zool. Beitr. 45:129-136.

Čerňanský, A., Syromyatnikova, E.V. 2021. The first pre-Quaternary fossil record of the clade Mabuyidae with a comment on the enclosure of the Meckelian canal in skinks. Pap. Palaeontol. 7(1):195-215.

Čerňanský, A., Klembara, J., Smith, K.T. 2016. Fossil lizard from central Europe resolves the origin of large body size and herbivory in giant Canary Island lacertids. Zool. J. Linn. Soc-Lond. 176(4):861-877.

Čerňanský, A., Bolet, A., Müller, J., Rage, J.C., Augé, M., Herrel, A. 2017. A new exceptionally preserved specimen of *Dracaenosaurus* (Squamata, Lacertidae) from the Oligocene of France as revealed by micro-computed tomography. J. Vert. Paleontol. 37(6):e1384738.

Čerňanský, A., Syromyatnikova, E.V., Kovalenko, E.S., Podurets, K.M., Kaloyan, A.A. 2020. The key to understanding the European Miocene Chalcides (Squamata, Scincidae) comes from Asia: the lizards of the East Siberian Tagay locality (Baikal lake) in Russia. Anat. Rec. 303(7):1901-1934.

Cox, S.C., Carranza, S., Brown, R.P. 2010. Divergence times and colonization of the Canary Islands by Gallotia lizards. Mol. Phylogenet. Evol. 56(2) :747-757.

Cruzado-Caballero, P., Castillo Ruiz, C., Bolet, A., Colmenero, J.R., De la Nuez, J., Casillas, R., Llacer, S., Bernardini, Fortuny, J. 2019. First nearly complete skull of

Gallotia auaritae (lower-middle Pleistocene, Squamata, Gallotiinae) and a morphological phylogenetic analysis of the genus *Gallotia*. Sci. Rep. 9(1) :1-14.

Evans, S.E. 2008. The skull of lizards and tuatara. In (Gans, C. ed.), Biology of the Reptilia. Volume 20: The Skull of Lepidosauria. Society for the Study of Amphibians and Reptiles, USA 1-347

Friebohle, J. 2019. Potential Methods for Control of the Invasive California Kingsnake (*Lampropeltis californiae*) in Gran Canaria, Canary Islands, Spain. (Master dissertation, Truman State University).

Garcia-Porta, J., Irisarri, I., Kirchner, M., Rodríguez, A., Kirchhof, S., Brown, J. L., Macleod, A., Turner, A.P., Ahmadzadeh, F., Albaladejo, G., Crnobrnja-Isailovic, J., De la Riva, I., Fawzi, A., Galán P., Göçmen, B., Harris, J., Jiménez-Robles, O., Joger, U., Jovanović Glavaš, O., Karış, M., Koziel, G., Künzel, S., Lyra, M., Miles, D., Nogales, M., Oğuz, M.A., Pafilis, P., Rancilhac, L., Rodríguez, N., Rodríguez Concepción, B., Sanchez, E., Salvi, D., Slimani, T., S'khifa, A., Qashqaei, A.T., Žagar, A., Lemmon, A., Moriarty Lemmon, E., Carretero, M.A., Carranza, S., Philippe, H., Sinervo, B., Müller, J., Vences, M., Wollenberg Valero, K. C. 2019. Environmental temperatures shape thermal physiology as well as diversification and genome-wide substitution rates in lizards. Nat. Commun. 10(1):1-12.

Gauthier, J.A., Kearney, M., Maisano, J.A., Rieppel, O., Behlke, A.D. 2012. Assembling the squamate tree of life: perspectives from the phenotype and the fossil record. Bull. Peabody Mus. Nat. Hist. 53(1) :3-308.

Hernández, E., Nogales, M., Martín, A. 2000. Discovery of a new lizard in the Canary Islands, with a multivariate analysis of *Gallotia* (Reptilia: Lacertidae). Herpetologica. 63-76.

Hutterer, R. 1985. Neue Funde von Rieseneidechsen (Lacertidae) auf der Insel Gomera. Bonn Zool. Beitr. 36(3/4):365-394.

Klembara, J., Böhme, M., Rummel, M. 2010. Revision of the anguine lizard *Pseudopus laurillardi* (Squamata, Anguidae) from the Miocene of Europe, with comments on paleoecology. J. Paleontol. 84:159-196.

Klembara, J., Hain, M., Dobiášová, K. 2014. Comparative anatomy of the lower jaw and dentition of *Pseudopus apodus* and the interrelationships of Species of Subfamily Anguinae (Anguimorpha, Anguidae). Anat. Rec. 297:516-544.

Kozlowski, J. 1996. Optimal allocation of resources explains interspecific life-history patterns in animals with indeterminate growth. Proc. R. Soc. B: Biol. Sci. 263:559-566.

Lehrs, P. 1914. Description of a new lizard from the Canary Islands. Proc. Zool. Soc. Lond. 1914:681-684.

López-Jurado, L.F. 1989. A new Canarian lizards subspecies from Hierro Island (Canarian archipelago). Bonn. Zool. Beitr. 40(3/4) :265-272.

Marcé-Nogué, J., Fortuny, J., Gil, L., Sánchez, M. 2015. Improving mesh generation in fnite element analysis for functional morphology approaches. Span. J. Paleontol. 30:117-132.

Mateo, J.A., García-Márquez, M., López-Jurado, L.F., Barahona, F. 2001. Descripción del lagarto gigante de La Palma (Islas Canarias) a partir de restos subfósiles. Rev. Esp. Herp. 15:53-59.

Medina, F.M., Nogales, M. 2009. A review on the impacts of feral cats (*Felis silvestris* catus) in the Canary Islands: implications for the conservation of its endangered fauna. Biodivers. Conserv. 18(4) :829-846.

Mertens, R. 1942. *Lacerta goliath* n. sp., eine ausgestorbene Rieseneidechse von den Kanaren. Senckenbergiana 25:330-339.

Nogales, M., Rando, J.C., Valido, A., Martín, A. 2001. Discovery of a living giant lizard, genus *Gallotia* (Reptilia: Lacertidae), from La Gomera, Canary Islands. Herpetologica. 169-179.

Oelrich, T.M. 1956. The anatomy of the head of *Ctenosaura pectinata* (Iguanidae). Miscellaneous Publications, Museum of Zoology, University of Michigan 94:1-122.

Oudart, P. 1839. Zoologie. Reptiles. In: Webb and Berthelot (1835-l850), Zoologie, Vol. 2, 2ª parte, 1 table.

Palacios-García, S., Cruzado-Caballero, P., Casillas, R., Castillo Ruiz, C. 2021. Quaternary biodiversity of the giant fossil endemic lizards from the island of El Hierro (Canary Islands, Spain). Quat. Sci. Rev. 262:106961.

Pandolfi, L., Raia, P., Fortuny, J., Rook, L. 2020. Editorial: Evolving Virtual and Computational Paleontology. Front. Earth Sci. 8:591813. doi: 10.3389/feart.2020.591813

Peters, W., Doria, G. 1882. Note erpetologiche e descrizione di una nuova specie di *Lacerta* delle isolc Canarie. Ann. Mus. Civ. Stor. Nat. Giacomo Doria 18:431-434.

Piquet, J.C., López-Darias, M. 2021. Invasive snake causes massive reduction of all endemic herpetofauna on Gran Canaria. Proc. R. Soc. B 288:20211939. https://doi.org/10.1098/rspb.2021.1939

Rage, J.C., Augé, M. 2010. Squamate reptiles from the Middle Eocene of Lissieu (France): a landmark in the middle Eocene of Europe. Geobios 43:253–268.

Schenkel, E. 1901. Achter Nachtrag zum Katalog der herpetologischen Sammlung des Basler Museums. Ber. Verh. Nat.forsch. Ges. Basel, 13:142-199.

Steindachner, F. 1889. Bericht über eine von Prof. 0. Simonyi auf den Roques del Zalmor bei Hierro (Canarische Inseln) entdeckte neue Eidechsenart von auffallender Grösse, *Lacerta simonyi* Steind. Anz. d. Kaiserl. Akad. Wissensch. Wein, Math.-Naturwiss. Cl., 26.

Suárez, N.M., Betancor, E., Pestano, J. 2010. Isolation and characterization of microsatellite loci in the endangered lizard *Gallotia bravoana* and cross-species amplification in other Canarian *Gallotia*. Conserv. Genet. Resour. 2(1):265-268.

Tuniz, C., Bernardini, F., Cicuttin, A., Crespo, M.L., Dreossi, D., Gianoncelli, A., Mancini, L., Mendoza Cuevas, A., Sodini, N., Tromba, G., Zanini, F., Zanolli, C. 2013. The ICTP-Elettra X-ray laboratory for cultural heritage and archaeology. Nucl. Instrum. Methods. Phys. Res. B 711:106-110.

Villa, A., Delfino, M. 2019. A comparative atlas of the skull osteology of European lizards (Reptilia: Squamata). Zool J Linn Soc-Lond 187(3):829-928.

Figure captions

Figure 1. Hemimandible of *G. goliath* with the measurements and angle of the coronoid used in this study (see Table 1). Bone color codes: blue, dentary; purple, splenial; red, angular; green, coronoid; yellow, surangular; blue, articular. Scale bar= 10 mm.

Figure 2. Right hemimandibles of analyzed specimens. A-B, *G. bravoana* subadult; C-D, *G. intermedia*; E-F, *G. bravoana* adult; G-H, *G. stehlini*; I-J, *G. simonyi*; K-L, *G. goliath*. A, C, E, G, I and L, medial views. B, D, F, H, J and K, lateral views. Abbreviations: aiaf, anterior inferior alveolar foramina; alp, anterolateral process; amf, anterior mylohyoid foramen; amp, anteromedial process; dp, dorsal process; ds, dental shelf; gf, glenoid fossa; mf, mandibular fossa; nf, nutritional foramina; pdp, posterodorsal process; pmf, posterior mylohyoid foramen; pmp, posteromedial process; pvp, posteroventral process; rp, retroarticular process; sa, symphysial area; tr, tympanic ridge. Scale bars= 10 mm.

Figure 3. Dentary. A-C, *G. bravoana* subadult; D-F, *G. bravoana* adult; G-I, *G. intermedia*; J-L, *G. simonyi*; M-O, *G. stehlini*; P-R, *G. goliath*. A, D, G, J, M and P, dorsal views. B, E, H, K, N and Q, lateral views. C, F, I, L, O and R, medial views. Scale bars= 10 mm.

Figure 4. Splenial. A-B, *G. bravoana* subadult; C-D, *G. bravoana* adult; E-F, *G. intermedia*; G-H, *G. simonyi*; I-J, *G. stehlini*; K-L, *G. goliath*. A, C, E, G, I and K, lateral views. B, D, F, H, J and L, medial views. Scale bars= 10 mm.

Figure 5. Coronoid. A-B, *G. bravoana* subadult; C-D, *G. bravoana* adult; E-F, *G. intermedia*; G-H, *G. simonyi*; I-J, *G. stehlini*; K-L, *G. goliath*. A, C, E, G, I and K, medial views. B, D, F, H, J and L, lateral views. Scale bars= 10 mm.

Figure. 6. Angular. A-B, *G. bravoana* subadult; C-D, *G. bravoana* adult; E-F, *G. intermedia*; G-H, *G. simonyi*; I-J, *G. stehlini*; K-L, *G. goliath*. A, C, E, G, I and K, lateral views. B, D, F, H, J and L, medial views. Scale bars= 10 mm.

Figure 7. Surangular. A-B, *G. bravoana* subadult; C-D, *G. bravoana* adult; E-F, *G. intermedia*; G-H, *G. simonyi*; I-J, *G. stehlini*; K-L, *G. goliath*. A, C, E, G, I and K, lateral views. B, D, F, H, J and L, medial views. Scale bars= 10 mm.

Figure 8. Articular. A-C, *G. bravoana* subadult; D-F, *G. bravoana* adult; G-I, *G. intermedia*; J-L, *G. simonyi*; M-O, *G. stehlini*; P-R, *G. goliath*. A, D, G, J, M and P, dorsal views. B, E, H, K, N and Q, lateral views. C, F, I, L, O and R, medial views. Scale bars= 10 mm.

Table 1: Data obtained from the studied specimens. See Figure 1 for details of measurements.

Table 2: Maximum length of each bone. The length of the post-dental part of the mandible is measured between the end of the angular process of the dentary and the posterior end of the mandible.

Table 3. Length of each bone as a percentage of the total length of the mandible, without taking into account the overlap with other bones.

Table 4. List of characters with ontogenetic variation according to previous studies (Barahona (1996), Barahona and Barbadillo (1998), Barahona et al. (2000), Čerňanský et al. (2016) and Palacios-García et al. (2021)) and evaluated in the present study.

Table 5. List of characters with interspecific variation according to previous and present studies.

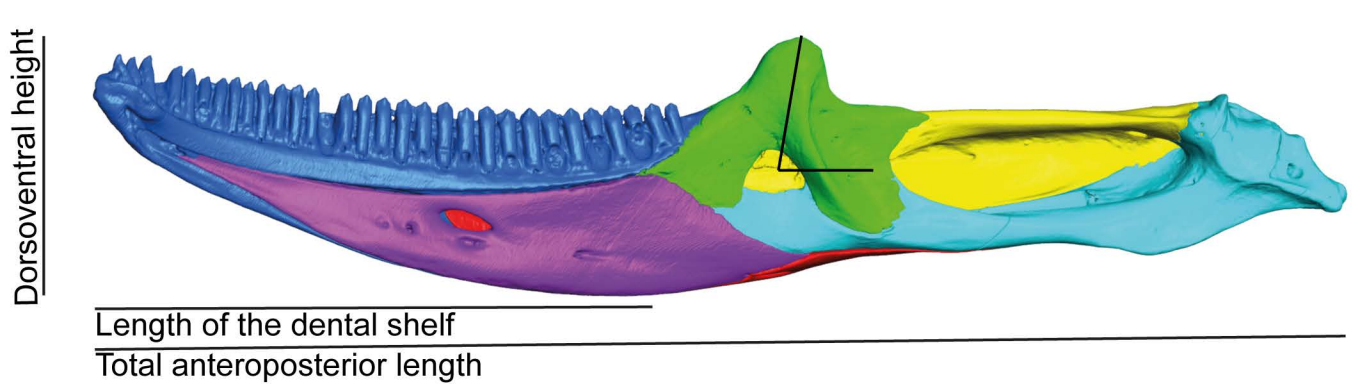
Dorsoventral height
Length of the dental shelf
Total anteroposterior length

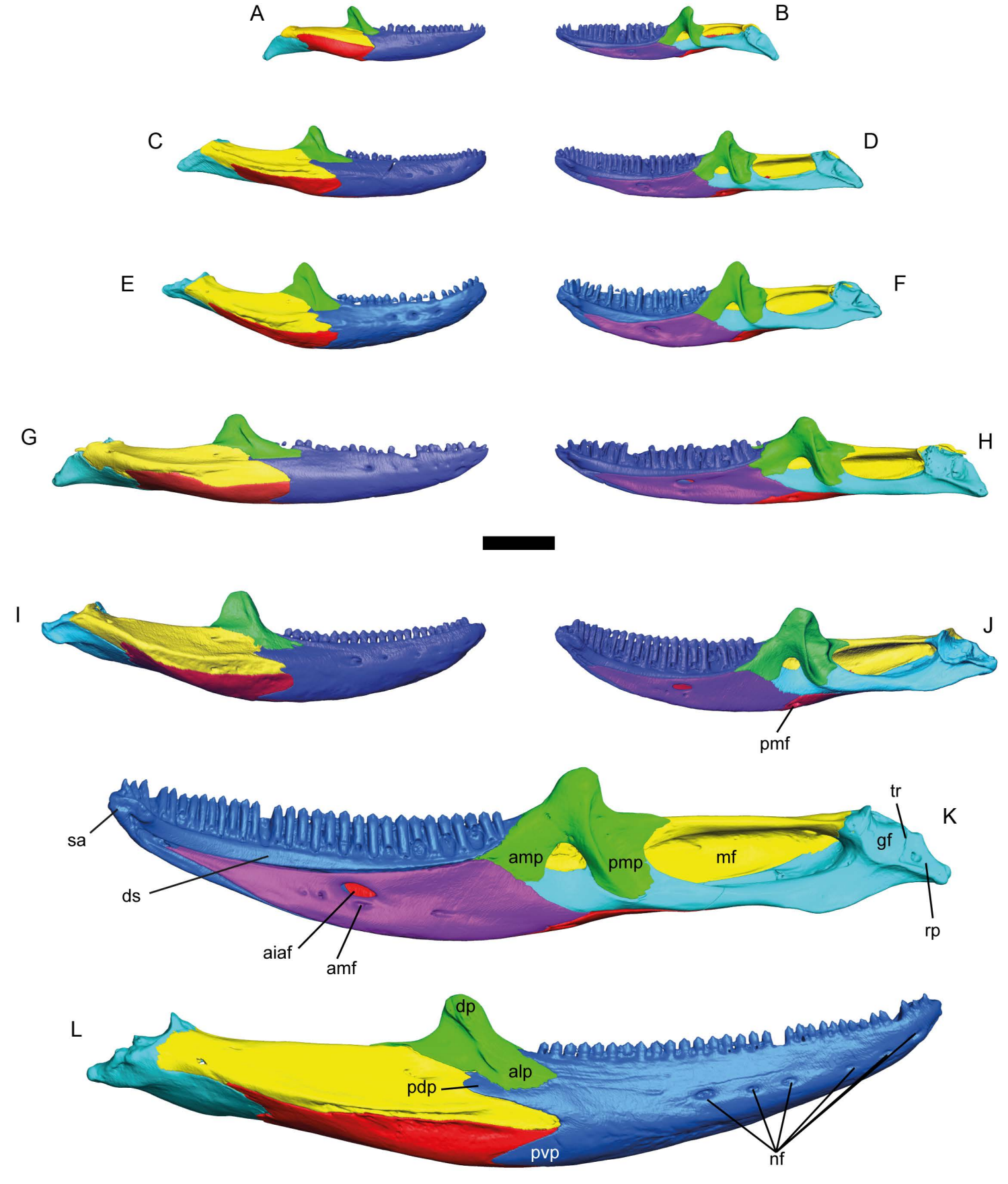
A
B
C
D
E
F
G
H
I
J
pmf
sa
ds
aiaf
amf
amp
pmp
mf
tr
gf
rp
K
L
dp
alp
pdp
pvp
nf

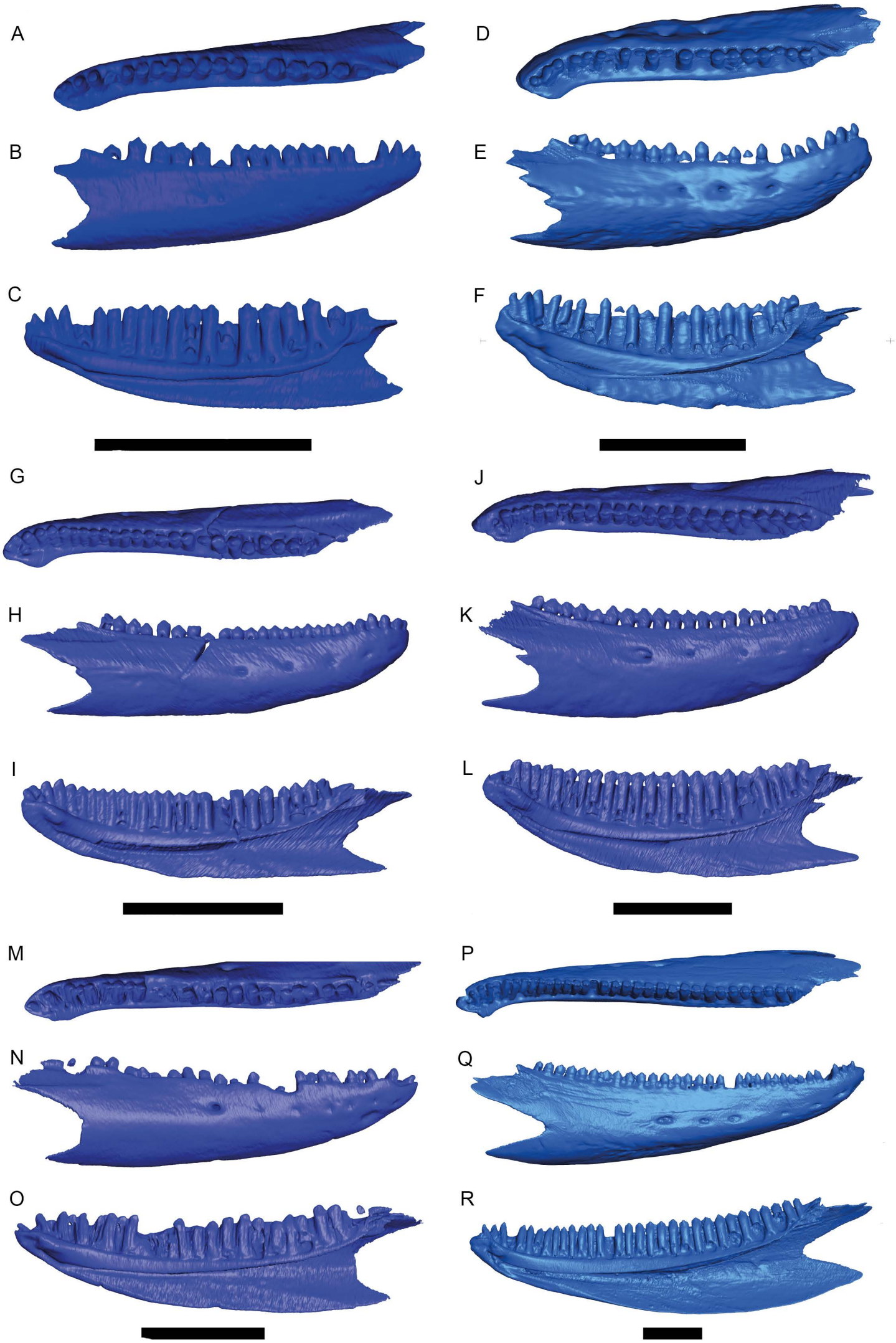
A
B
C
D
E
F
G
H
I
J
K
L
M
N
O
P
Q
R

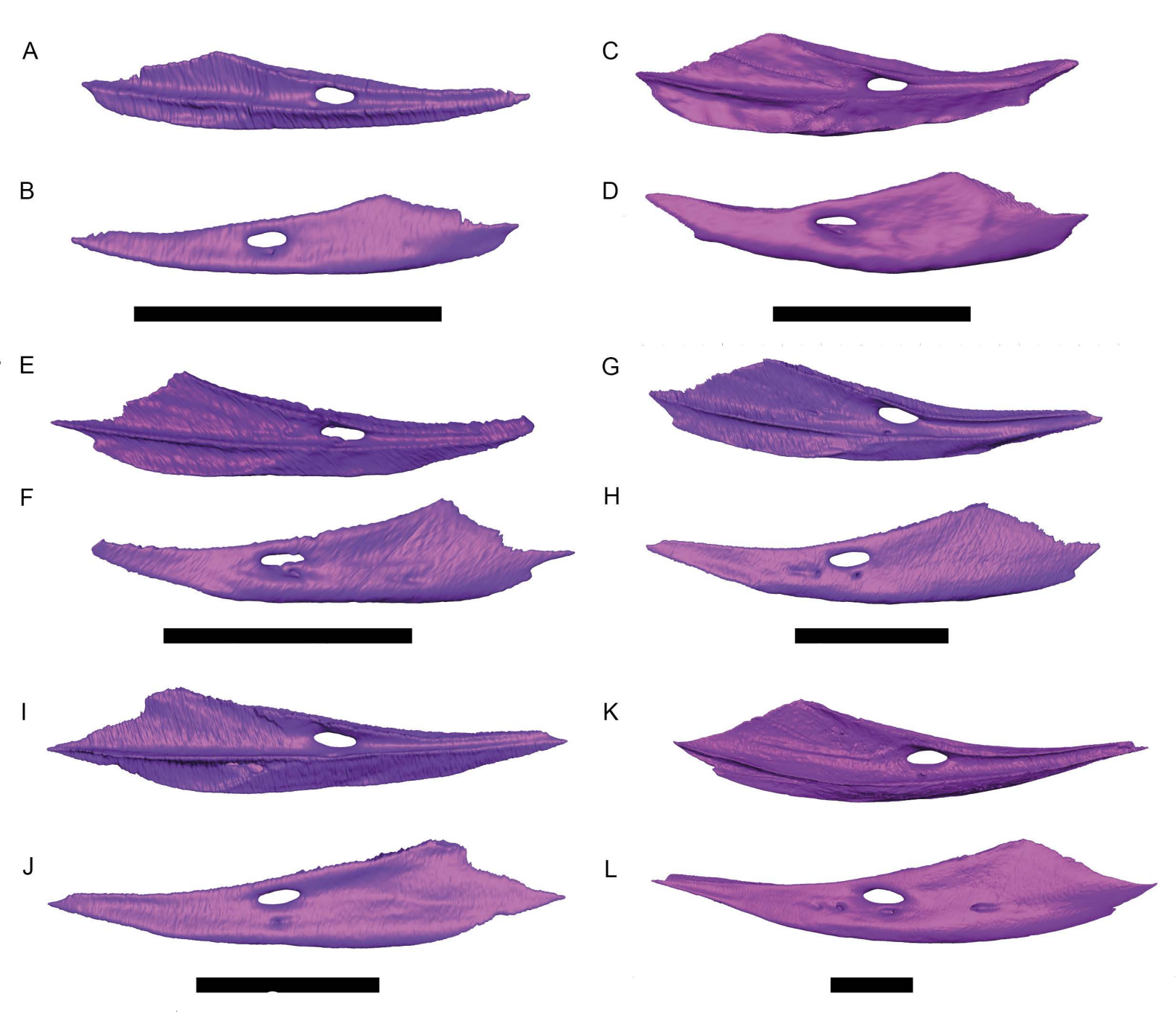
A
B
C
D
E
F
G
H
I
J
K
L

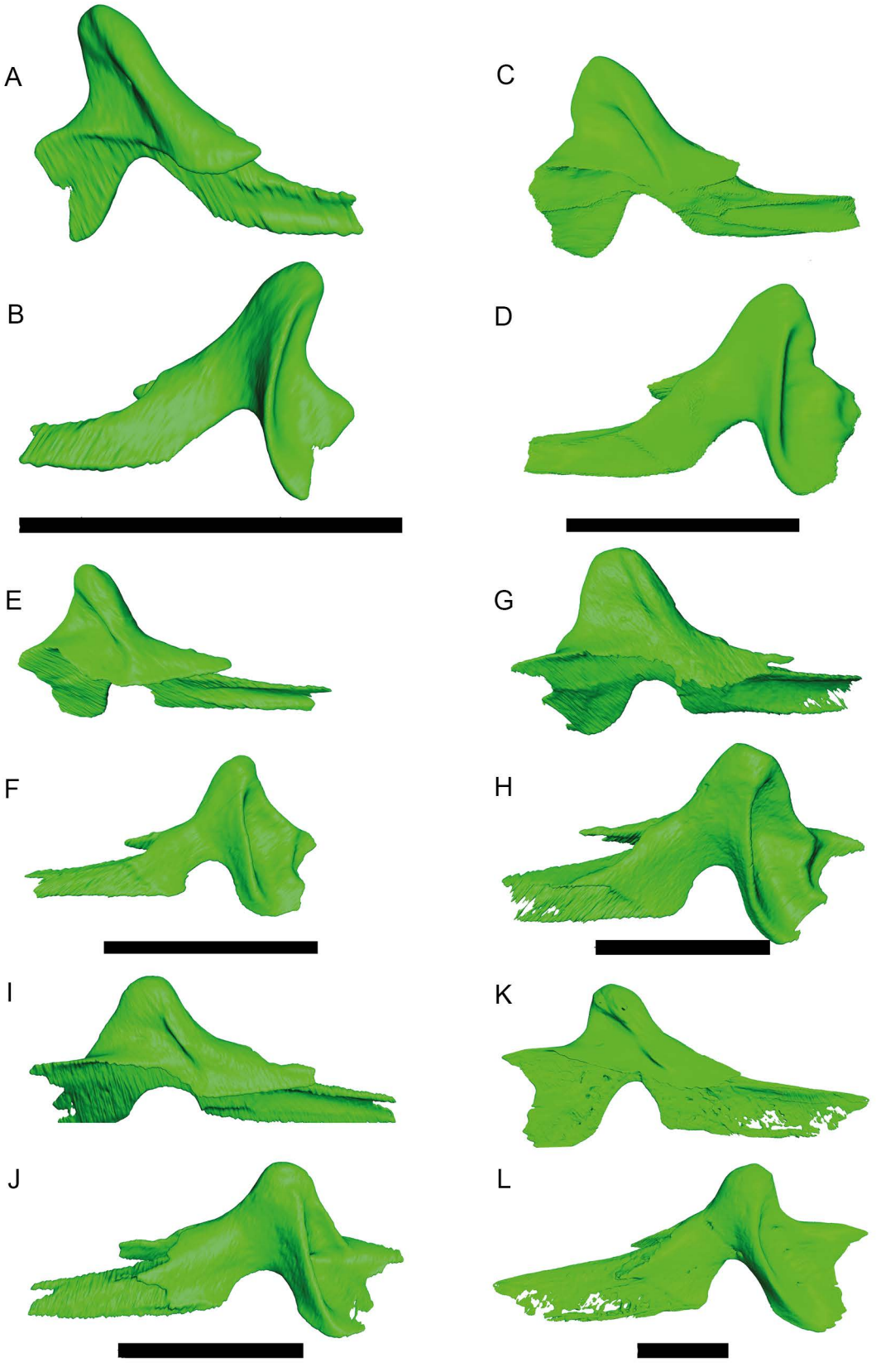
A
C
B
D
E
G
F
H
I
K
J
L

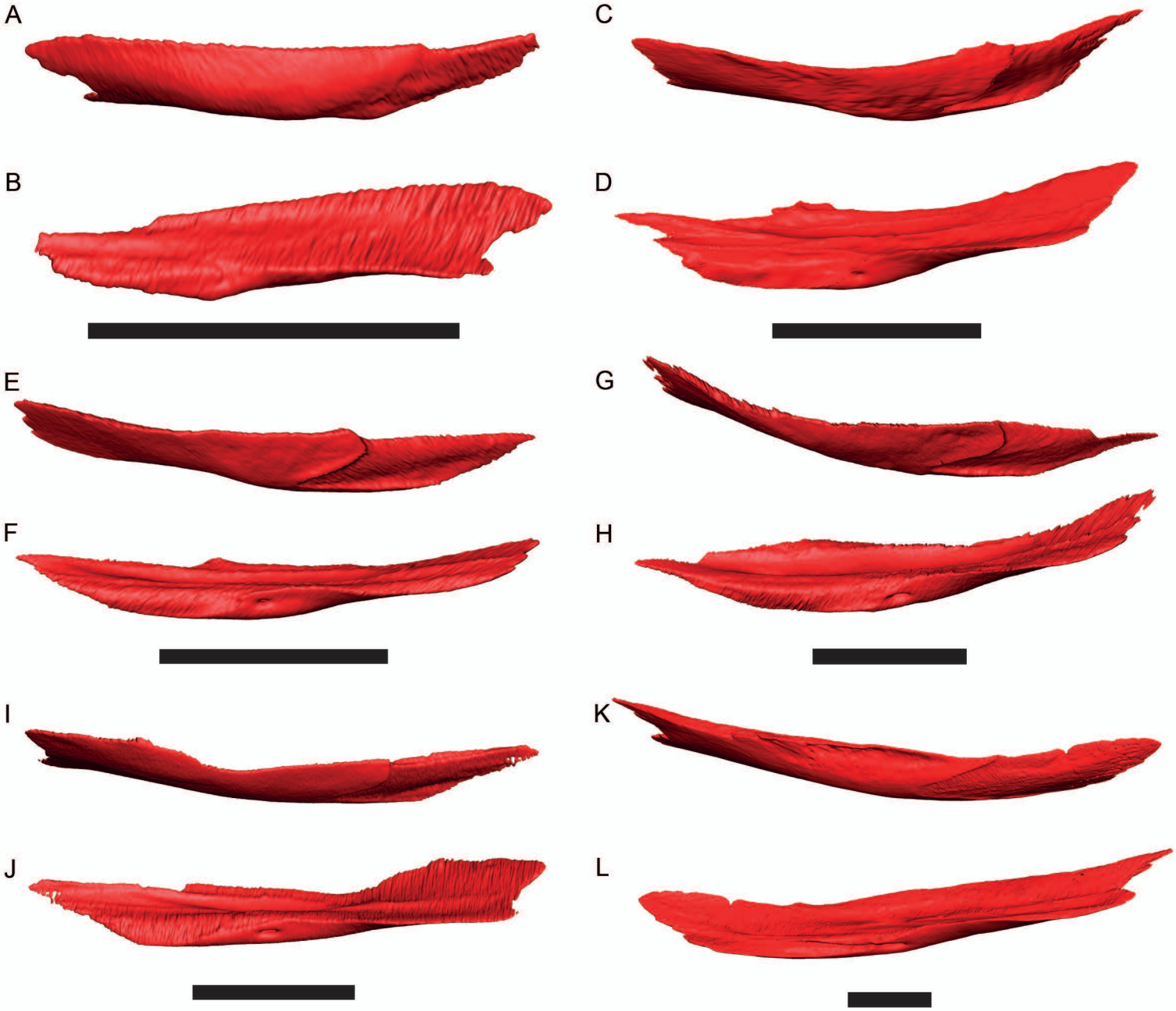
A
C
B
D
E
G
F
H
I
K
J
L

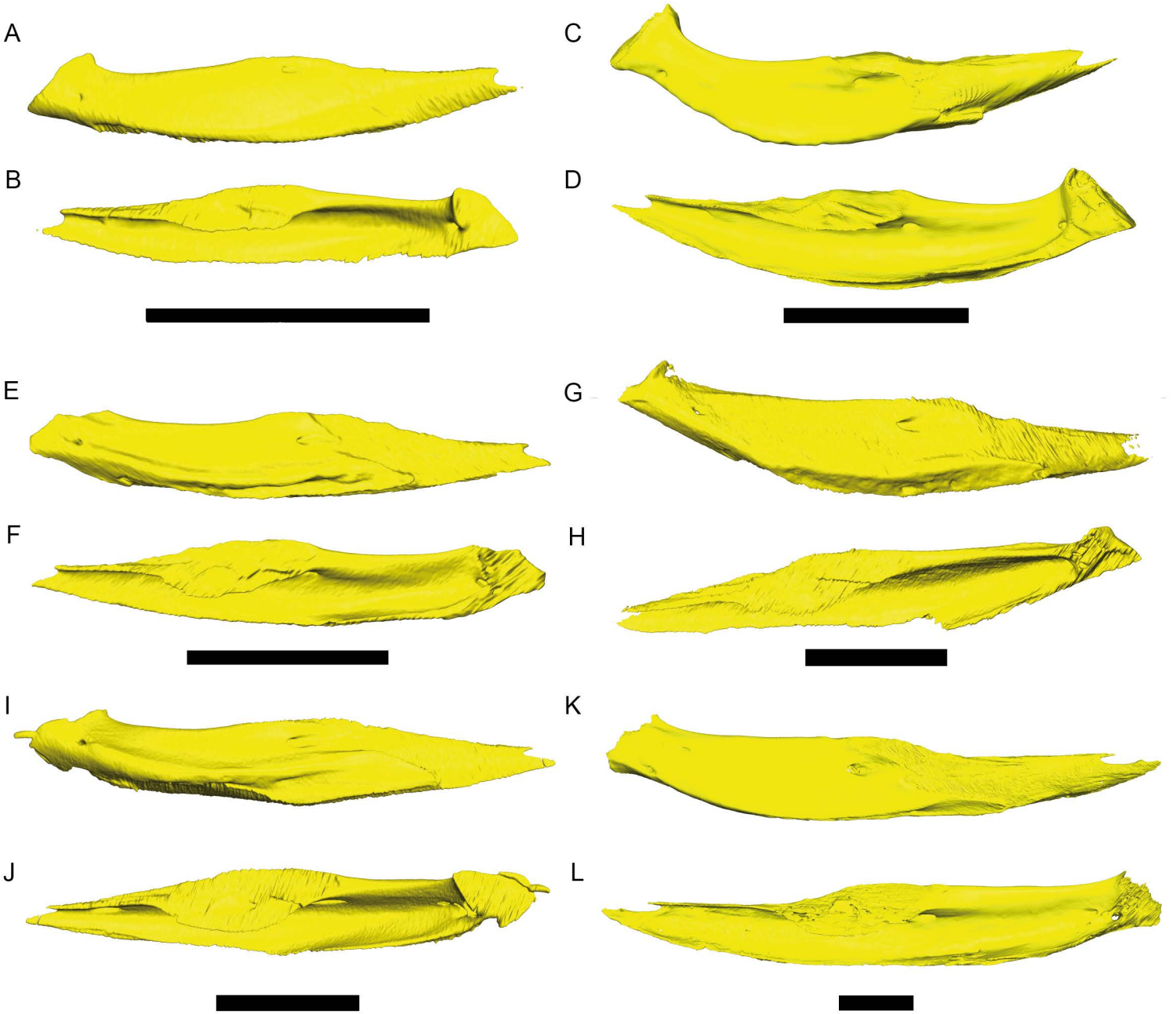
A
B
C
D
E
F
G
H
I
J
K
L

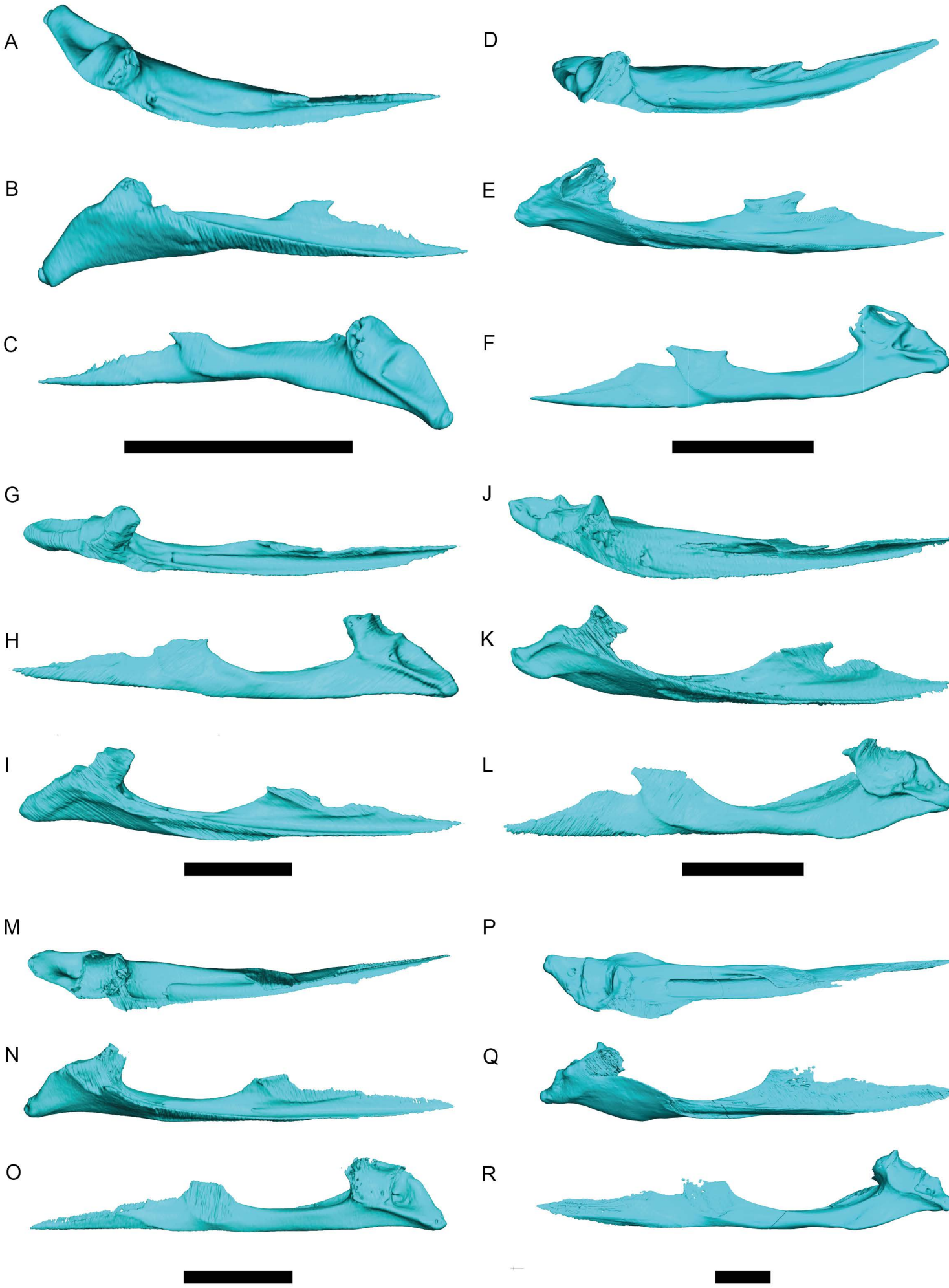
A
D
B
E
C
F
G
J
H
K
I
L
M
P
N
Q
O
R

Sizes (mm)	***G. goliath*** PCCRULL1195	***G. bravoana*** PCCRULL1250 (Subadult)	***G. bravoana*** PCCRULL1251	***G. intermedia*** DZUL-2208	***G. simonyi*** CRLGH Gs-1/2015	***G. stehlini*** TFMV-VT96
Total anteroposterior length of the mandible	119.0	31.1	44.8	42.7	61.0	60.5
Dorsoventral height of the mandible	24.0	8.1	11.8	9.1	14.9	12.2
Length of the dental shelf	57.2	14.9	20.1	19.4	27.9	28.4
Number of dentary teeth positions	32	19	21	25	23	27

Nº teeth/mm	0.6	1.3	1.1	1.3	0.8	0.9
Nº labial foramina in the dentary	6	6	7	5	7	7
Location anterior mylohyoid foramen	22^{th} tooth position	15^{th} tooth position	$13\text{-}14^{th}$ tooth position	$18\text{-}19^{th}$ tooth position	$15\text{-}17^{th}$ tooth position	$18\text{-}20^{th}$ tooth position

Table 1: Data obtained from the studied specimens. See figure 1 for details about measurements.

Length (mm)	***G. goliath*** PCCRULL1195	***G. bravoana*** PCCRULL1250 (Subadult)	***G. bravoana*** PCCRULL1251	***G. intermedia*** DZUL-2208	***G. simonyi*** CRLGH Gs-1/2015	***G. stehlini*** TFMV-VT96
Postdentary section of the mandible.	51.5	14.5	20.5	18.3	28.5	28.1
Dentary	67.5	17.6	24.5	24.4	32.8	33.1
Splenial	65.7	14.6	22.2	19.5	29.7	28.4
Coronoid	28.4	8.5	14.1	14.3	19.9	20.8
Surangular	56.7	17.3	27.8	25.7	38.1	37.1
Angular	59.4	14.1	25.3	23.0	34.7	32.2
Articular	77.2	18.4	30.2	27.9	38.6	39.6

Table 2: Maximum length of each of bone. The length of the post-dental part of the mandible is measured between the end of the angular process of the dentary and the posterior end of the mandible.

% bone vs total anteroposterior length	***G. goliath*** PCCRULL1195	***G. bravoana*** PCCRULL1250 (Subadult)	***G. bravoana*** PCCRULL1251	***G. intermedia*** DZUL-2208	***G. simonyi*** CRLGH Gs-1/2015	***G. stehlini*** TFMV-VT96
Dentary	56.7	56.7	54.7	57.2	53.8	54.7
Splenial	55.2	47.0	49.6	45.7	48.7	46.9
Coronoid	23.8	27.3	31.5	33.4	32.7	34.4
Surangular	47.7	55.9	62.0	60.2	62.4	61.4
Angular	50.0	45.3	56.5	53.8	56.8	53.2
Articular	64.8	59.4	67.3	65.4	63.2	65.5

Table 3. Percentage of length of each bone versus the total length of the mandible without taking into account the overlap with other bones.

Characters with ontogenetical signal according to previous studies	**Yes**	**No**	**Present study**
Number and location of the labial foramina.	All species.		
The posteroventral process of the dentary is longer than the posterodorsal process in juveniles. In adults this character is the other way around.	*G. galloti*, *G. simonyi* and *G. stehlini.*	In *G. caesaris* and *G. atlantica,* both process have similar length. In *G. goliath,* the posterodorsal process is slightly longer than the posteroventral process in juvenile specimens, whereas in adult individuals the two processes are of more similar length.	*G. bravoana* subadult and adult and in *G. simonyi* both processes have similar length.
Fusion of the articular and surangular.	*G. galloti*		In *G. stehlini* and *G. bravoana* the bones are not fused.

			G. simonyi and *G. intermedia* present fused bones only at the posterior end. *G. bravoana* subadult the bones are not fused, although it cannot be ruled out.
A posteriorly inclined dorsal process of the coronoid.	*G. galloti*		*G. goliath* and *G. bravoana* subadult are inclined. *G. simonyi, G. stehlini, G. bravoana* adult and *G. intermedia* are straight.
A short or poorly developed anteromedial process of the coronoid.	All species.		

A shallow adductor fossa of the coronoid.			In *G. bravoana* subadult, the fossa is shallow, whereas in the rest of specimens is deep.
Opening of the anterior inferior alveolar foramen of the splenial.			*G. bravoana* subadult has this foramen partially open whereas in the adult specimen is close. *G. goliath, G. stehlini* and *G. simonyi* have completely open the foramen. *G. intermedia* has this foramen partially open.
Absence of the dorsal depression of the surangular in lateral view			*G. bravoana* subadult does not have this depression. The rest of species has this depression.

The ventral margin of the articular goes from straight in juveniles to bulging in adults.	*G. stehlini* and *G. simonyi*.		*G. bravoana*
Number of cuspids in the dentary teeth.	*G. stehlini* and *G. simonyi*.	*G. bravoana* and *G intermedia*	
Articular areas of the mandible undergo progressive ossification.	In *G. galloti*, the last in ossify is the area of articulation between the mandible and the quadrate.	*G. stehlini* and *G. simonyi* lack or delay of ossification of the posterior aspect of the surangular by pedamorphosis.	

Table 4. List of characters with ontogenetic variation according to previous studies (Barahona (1996), Barahona and Barbadillo (1998), Barahona et al. (2000), Čerňanský et al. (2016) and Palacios-García et al. (2021)) and evaluated in the present study.

Characters with interspecific signal according to previous studies	Character description	Character value	Taxon	Reference
Dentary	Number of dentary teeth positions.	36	*G. goliath*	Bravo (1953).
		30-32		Castillo et al (1994).
		32		Cruzado-Caballero et al. (2019).
		18-35		Palacios-Garcia et al. (2021).
		32	*G. auaritae*	Mateo et al. (2001).
		18-33		Mateo (2009).
		27		Cruzado-Caballero et al (2019).

20-26	*G. simonyi*	Castillo et al (1994).
17-24		Rodriguez et al. (1998).
17-25		Palacios-Garcia et al. (2021).
23		Present study.
21-26	*G. bravoana*	Hutterer (1985); Nogales et al. (2001).
27		Mateo et al. (2011).
19		Present study.
16-29	*G. stehlini*	Castillo et al (1994).
16-27		Barahona et al. (2000).
27		Present study.

	25	*G. intermedia*	Cruzado-Caballero et al. (2019). Present study.
Number of cuspid in dentary teeth.	Mono-. bi- or tricuspids.	*G. galloti, G. atlantica, G. caesaris, G. simonyi, G. bravoana, G. goliath, G. auaritae, G. intermedia.*	Boulenger (1891); Machado (1985); Hutterer (1985); López-Jurado and Mateo (1995); Barahona et al. (2000); Hernández et al. (2000); Nogales et al. (2001); Mateo et al (2001; 2011). Present study.
	Tetracuspid to six cuspids.	*G. goliath*	Mertens (1942); Bravo (1953); Palacios-Garcia et al. (2021).

		G. simonyi, máximum tetracuspid.	Palacios-Garcia et al. (2021).
		G. stehlini	López-Jurado and Mateo (1995); Barahona et al. (2000); Nogales et al. (2001).
End of posterodorsal process.	Not surpasses the apex of the coronoid.	*G. stehlini*, *G. bravoana*, *G. simonyi*, *G. goliath.*	Present study.
	Surpasses the apex of the coronoid.	*G. intermedia*	Present study.
Shape of the end of the posterodorsal process.	Present small projections.	One dorsal projection in *G. goliath*, one dorsal projection and one ventral projection in *G. simonyi* and *G. bravoana.*	Present study.

		Without small projections.	*G. intermedia* and *G. stehlini.*	Present study.
Coronoid	Shape of the posteromedial process.	Concave posterior border.	*G. goliath, G. bravoana* and *G. intermedia.*	Present study.
		S-shaped.	*G. stehlini* and *G. simonyi.*	Present study.
	S-shaped dorsoventral crest in the posteromedial process.	Presence.	*G. intermedia, G. bravoana* and *G. simonyi.*	Present study.
		Absence.	*G. goliath* and *G. stehlini.*	Present study.
Splenial	Anterior inferior alveolar foramen.	Completely open.	*G. goliath, G. stehlini* and *G. simonyi.*	Present study.
		Close.	*G. bravoana* adult.	Present study.
Surnagular-articular	Degree of fusion.	Not fused.	*G. bravoana* and *G. stehlini.*	Present study.

		Partially fused.	*G. intermedia* and *G. simonyi.*	Present study.
Articular	Direction of the retroarticular process with respect to the ventral border of the surangular.	Straight.	*G. intermedia* and *G. stehlini.*	Present study.
		Dorsal.	*G. goliath, G. bravoana* and *G. simonyi.*	Present study.
Mandible	Degree of curvature with respect to the axial axis.	Pronounced.	*G. goliath*, *G. simonyi* and *G. bravoana.*	Present study.
		Intermediate.	*G. intermedia* and *G. stehlini.*	Present study.

Table 5. List of characters with interspecific variation according to previous and present studies.